

光学学报

724 W, 0.9 mJ, 227 fs 四通道相干合成超快光纤激光系统(特邀)

王志浩¹, 彭双喜¹, 徐浩¹, 李政言², 张庆斌^{1,3*}, 陆培祥^{1,3}

¹华中科技大学武汉光电国家研究中心与物理学院, 湖北 武汉 430074;

²华中科技大学光学与电子信息学院, 湖北 武汉 430074;

³湖北光谷实验室, 湖北 武汉 430074

摘要 报道了一种基于四通道光纤放大器相干光束合成的高功率飞秒激光系统。每个通道均采用大模场棒状光子晶体光纤, 平均功率达到 220 W。通过稳定的主动相位锁定技术, 压缩后的激光系统在 800 kHz 的重复频率下实现了 724 W 的平均功率和 0.9 mJ 的单脉冲能量。合成后的激光保持了良好的光束质量和功率稳定性, 合束光斑的光束质量因子 $M^2 < 1.25$, 功率波动的均方根误差为 0.59%。此外, 通过优化各通道放大器的增益并测量分析压缩后脉冲的时域特性, 实现了对放大前脉冲的精确色散预补偿。本系统在没有使用脉冲整形或者光谱调制的情况下, 实现了脉冲宽度从 445 fs 到 227 fs 的优化。

关键词 超快光纤激光器; 相干光束合成; 哨啾脉冲放大; 色散补偿

中图分类号 TN248

文献标志码 A

DOI: 10.3788/AOS241138

1 引言

高平均功率、高重复频率的超快激光器已经在工业和科学领域得到广泛的应用, 例如材料的切割和高速微加工, 高次谐波的产生, 以及太赫兹辐射^[1-6]。镱掺杂作为增益介质的板条、碟片和光纤激光器, 因其低量子缺陷和优越的散热性能, 成为实现高平均功率激光输出的有效工具^[7-11]。其中, 板条和碟片激光器在产生高单脉冲能量方面占据优势, 而光纤激光器则能够实现更高的平均功率和更大的增益带宽, 支持更短的脉冲宽度。然而, 进一步提升激光单脉冲能量和平均功率仍面临物理过程的限制和技术瓶颈^[12]。光纤激光器的主要限制因素是放大过程中过多累积的非线性相移和横模不稳定现象^[13-14]。将大模场面积(LMA)光纤^[15]和啁啾脉冲放大(CPA)技术^[16]相结合, 可以有效降低激光脉冲在光纤中的峰值强度, 减弱放大过程的非线性效应, 从而获得更高的平均功率和单脉冲能量。此外, 多模光纤中的光束自清洁现象可有效克服光束畸变, 显著提升多模光束的光束质量, 有望解决横模不稳定现象带来的光束质量退化问题^[17-18]。尽管如此, 受限于光纤制备的工艺水平以及 CPA 中大尺寸衍射光栅的空间尺寸和成本, 进一步提升单个光纤激光放

大器的平均功率和脉冲能量仍面临挑战。

相干光束合成(CBC)是一种在保持光束质量的同时, 拓展平均功率和单脉冲能量上限的有效手段。在典型的 CBC 结构中, 种子光被分到 N 路放大器中, 并在每一路中被放大至单个放大器的极限, 随后通过相干叠加合成单个光束。理论上, 合束后的激光功率和能量可达到单个放大器的 N 倍。然而, 在实际应用中, 由于光斑质量的差异以及光束时空间特性的偏差, 合成过程中会产生功率损耗, 这一损耗可通过合束效率量化。为了维持 N 路光束稳定的相干叠加状态, 还需要采用主动的相位控制技术来保持光束之间的相位稳定^[19-20]。CBC 的概念最早被应用于连续光和长脉冲^[21-23], 随后扩展到飞秒脉冲领域^[24-25]。CBC 可以应用于多种激光器结构中, 但光纤激光器的波导结构使得不同通道中的光束的时空特性具有更高的可重复性, 因此其表现尤为突出。近期, 已有研究团队通过 8 通道和 16 通道光纤激光器 CBC 实现了平均功率为 1 kW、单脉冲能量为 1 mJ、平均功率为 1 kW、单脉冲能量为 10 mJ 的激光输出^[26-27]。此外, 通过将时间合成与空间合成相结合, 640 W 的平均功率、32 mJ 的单脉冲能量得以实现^[28]。在这些工作中, 单个光纤放大器的平均功率一般在 100 W 附近。因此, 为了实现 kW

收稿日期: 2024-06-06; 修回日期: 2024-07-05; 录用日期: 2024-07-18; 网络首发日期: 2024-07-28

基金项目: 国家自然科学基金(92150106, 12021004, 11934006)、湖北省重大项目(JD)(203BAA015)、光谷实验室创新项目(OVL2021ZD001)、华中科技大学交叉研究支持计划(2023JCYJ041)

通信作者: *zhangqingbin@hust.edu.cn

级激光输出,通常需要数十路激光的相干合成。另一方面,由于多级啁啾脉冲放大过程的增益窄化和压缩过程的高阶色散无法完全补偿,压缩后的脉冲宽度通常超过300 fs且难以达到傅里叶变换极限(TL)脉宽。尽管通过空间光相位调制、光谱整形和后压缩等方法可以进一步优化脉冲宽度,但这些方法同时也增加了系统的复杂程度。

近期,本团队通过两通道光纤激光器的CBC实现了400 W、500 μJ、260 fs的激光输出^[29]。本文通过四通道CBC将激光系统的输出脉冲能量提升至近毫焦量级,同时保证了装置的紧凑性和扩展性。激光输出光斑质量良好,功率和相位具有较好的稳定性。此外,利用自制的二次谐波产生频率分辨光门(SHG-FROG),表征了压缩后激光脉冲的时域特性,分析了光谱相位和残留的高阶色散,并利用可调谐脉冲展宽器(TPSR)进行精确色散预补偿,最终获得了脉冲宽度为227 fs的激光输出。

2 实验装置

四通道飞秒光纤相干光束合成系统的实验装置

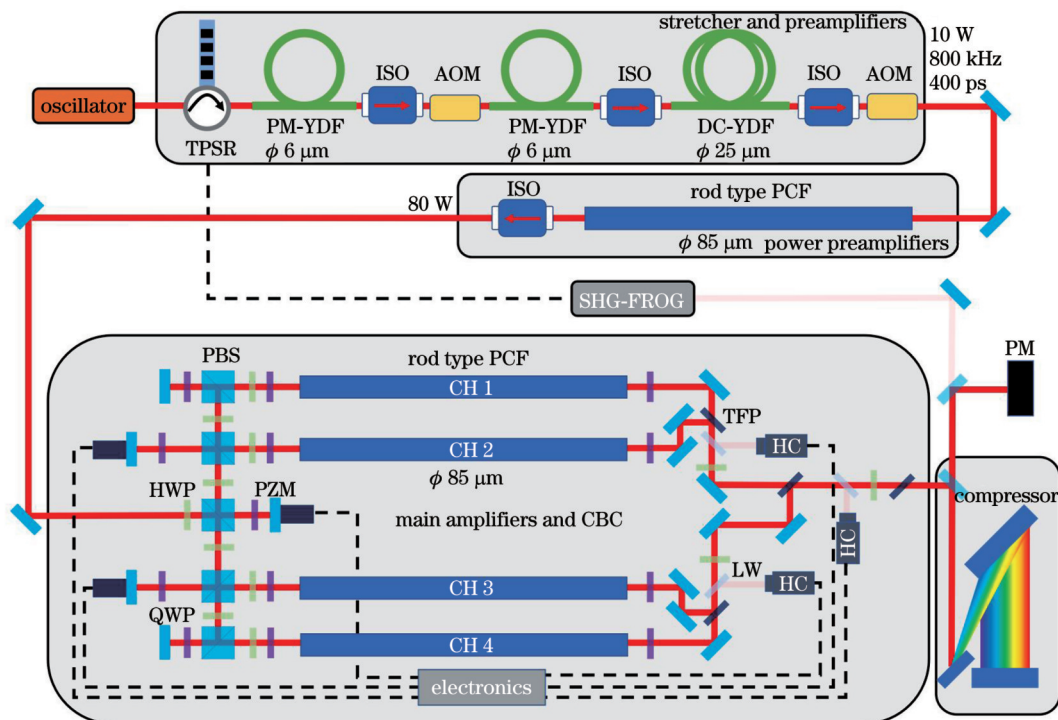


图1 实验装置示意图(TPSR代表可调谐脉冲展宽器,PM-YDF代表保偏掺镱光纤,DC-YDF代表双包层掺镱光纤,ISO代表光隔离器,AOM代表声光调制器,PCF代表光子晶体光纤,HWP代表半波片,QWP代表1/4波片,PBS代表偏振分光棱镜,PZM代表压电促动反射镜,TFP代表薄膜偏振片,LW代表窗片,PM代表功率计,SHG-FROG代表二次谐波产生频率分辨光门)

Fig. 1 Schematic diagram of experimental setup (TPSR represents tunable pulse stretcher, PM-YDF represents polarization-maintaining Yb-doped fiber, DC-YDF represents double-clad Yb-doped fiber, ISO represents isolator, AOM represents acousto-optic modulator, PCF represents photonic crystal fiber, HWP represents half-wave plate, QWP represents quarter-wave plate, PBS represents polarizing beam-splitter, PZM represents piezo-driven mirror, TFP represents thin film polarizer, LW represents laser window, PM represents power meter, and SHG-FROG represents second harmonic generation frequency resolved optical gating)

如图1所示。种子光源为锁模掺镱光纤振荡器,在40 MHz的重复频率下输出光谱的带宽为17 nm,脉冲宽度约为800 fs。使用带宽为15 nm的双啁啾光纤布拉格光栅(CFBG)组成的TPSR可提供41.6 ps²的2阶色散、-2.2 ps³的3阶色散以及0.1 ps⁴的4阶色散,将脉冲展宽至约1.1 ns。利用3级预放大和2级声光调制器降低重复频率后,输出中心波长为1035 nm、平均功率为10 W、脉冲宽度为400 ps、重复频率为800 kHz的激光。脉冲宽度的减小是由于增益窄化的影响^[30]。前2级预放大采用保偏单模掺镱光纤(PM-YSF-HI),长度分别为1 m和1.5 m;第3级预放大采用长度为4 m的双包层掺镱光纤(YB1200-25/250DC-PM)。随后,种子光通过棒状光子晶体光纤,在中心波长为976 nm、平均功率为150 W的半导体激光器反向泵浦下放大至约80 W。大模场棒状光子晶体光纤的纤芯直径为85 μm,数值孔径(NA)约为0.01,包层直径为260 μm,长度为0.8 m。之后利用波片和偏振分光棱镜(PBS)在空间上将种子光均等分为4个子脉冲,子脉冲在棒状光子晶体光纤主放大级中通过反向泵浦并行放大。为了精细控制4个通道之间的相位差,3个工

作频率为100 Hz的压电促动反射镜被配置在分束光路上。

为了最小化非线性相位累积并改善输出光束质量,在功率预放大器和主放大器中均使用圆偏光进行放大。经放大输出后,4路光束经由薄膜偏振片(TFP)进行两两合束。每次合成后,使用镀增透膜的窗片对光束进行采样,将采样光输入至Hänsch-Couillaud(HC)^[31]探测器中进行相对相位的计算,并将误差信号反馈至压电促动反射镜上,以实现相位的稳定控制,从而保证稳定的高功率相干激光输出,最终合成后的激光扩束到直径约为6 mm,通过一对反向平行放置、间距可调、刻线周期为1740 line/mm的衍射光栅进行色散补偿和脉冲压缩,光栅尺寸为25 mm×120 mm。压缩后的光束经过采样后输入到自制的SHG-FROG系统中进行时域特性诊断,并通过TPSR对种子光色散进行预补偿,实现进一步的脉冲压缩优化。

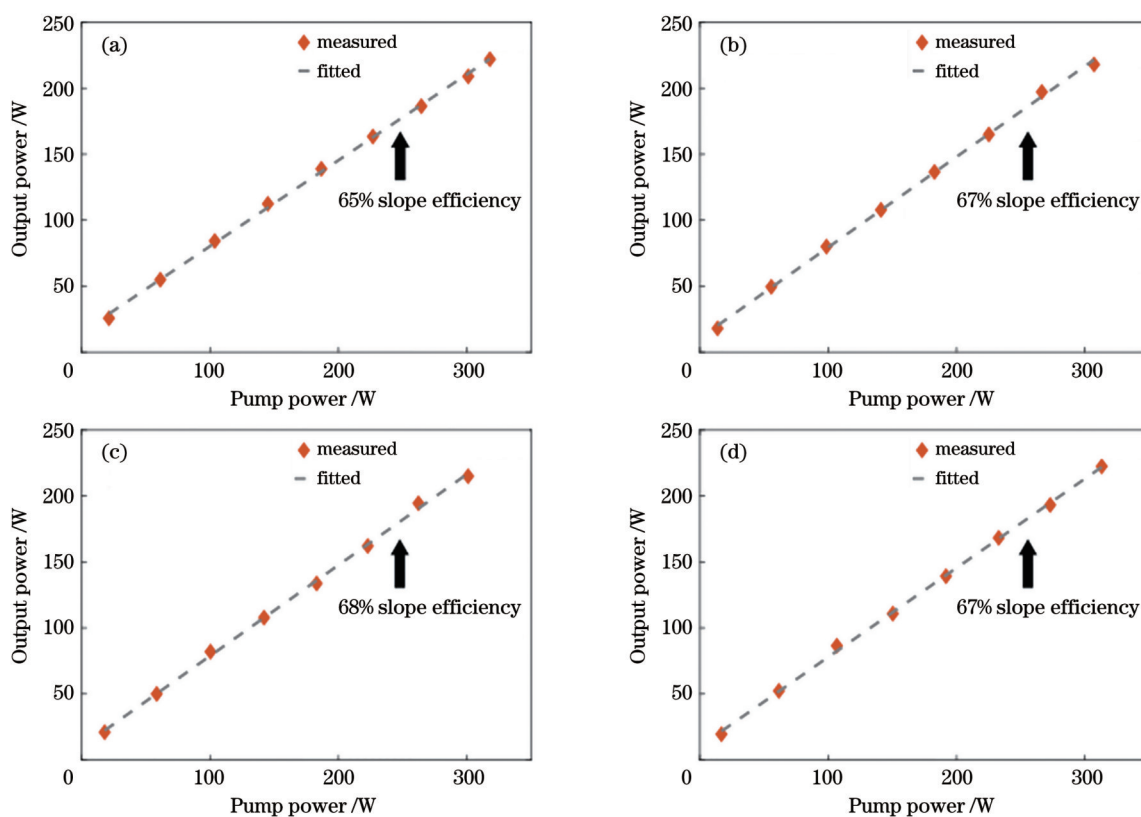


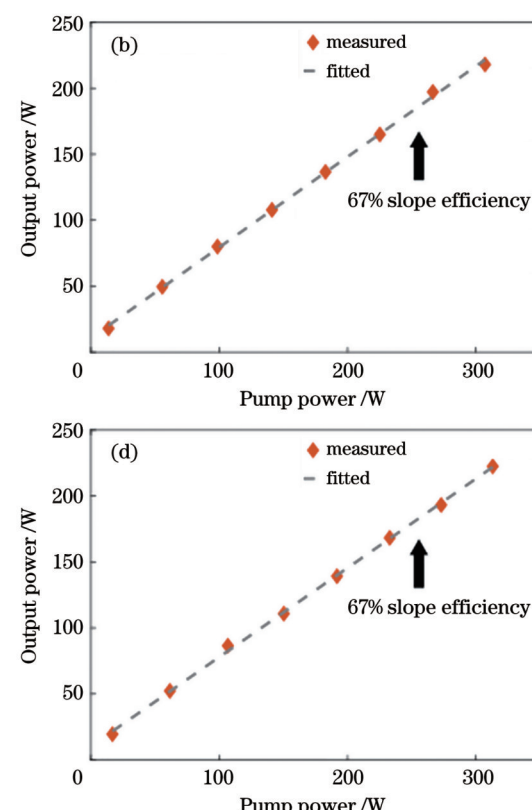
图2 四通道输出功率与各自泵浦光功率之间的函数曲线。(a)通道1;(b)通道2;(c)通道3;(d)通道4

Fig. 2 Output power as a function of pump power of each channel. (a) Channel 1; (b) channel 2; (c) channel 3; (d) channel 4

合成后的激光功率稳定性曲线如图3(a)所示。在前60 s内,由于相位稳定系统未开启,大气湍流、机械振动和高功率放大时的热漂移等因素导致各通道之间存在随机抖动的相位误差,无法形成有效的相干叠加。为了保证高功率相干合成激光输出,使用实时高效反馈的相位稳定系统是有必要的。在每次合束后,

3 实验结果与分析

为了确保高合成效率和接近变换极限的压缩脉冲,所有主放大器中的非线性相位必须匹配,因此四通道放大器均使用相近的种子光和泵浦光条件。各通道放大器的功率放大曲线如图2所示。在320 W功率的单通道激光泵浦下,各通道的输出平均功率在215 W到222 W之间,放大的拟合斜效率均达到65%以上,各通道之间的拟合斜效率差异最大不超过3%。由于激光放大使用了非保偏棒状光子晶体光纤,在功率放大过程中观察到非线性偏振旋转(NLPR)现象。这不仅降低了单个光束的偏振度,也不利于提高合束效率。通过调节放置于各通道放大器之前的半波片和1/4波片,改善了非线性偏振旋转问题,使各通道激光的偏振消光比达到15 dB以上。此外,通过控制各通道放大器的泵浦功率,以减小各通道激光的非线性相位差异,尽管这导致各路激光的放大功率有所偏差,但通过调节合束后的半波片,仍能保证较高的合束效率。



通过HC探测器实时探测和计算相对相位差,并通过纳米精度位移的压电促动反射镜进行补偿。相位稳定结果如图3(b)~(d)所示。在60 s内:通道1和2之间相位稳定时的锁相残差(σ)为25.23 mrad,对应于波长的1/249;通道3和4之间相位稳定时的锁相残差为19.38 mrad,对应于波长的1/324。最后,将相位稳定

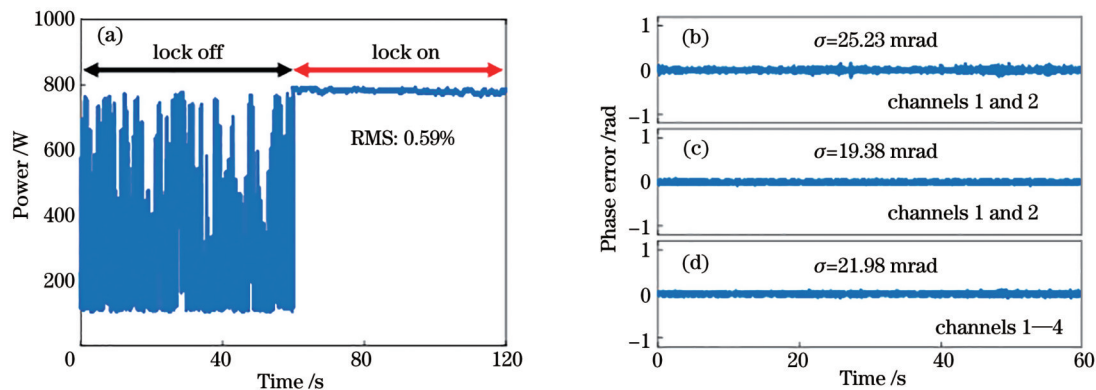


图3 合成光束的功率稳定性和相位稳定性。(a)功率稳定性;(b)通道1和2、(c)通道3和4,以及(d)通道1~4在开启相位稳定系统后的相位误差

Fig. 3 Power stability and phase stability of combined beams. (a) Power stability; phase error of (b) channels 1 and 2, (c) channels 3 and 4, and (d) channels 1~4 after starting phase stabilization system

的通道12与34进行合成,其锁相残差为21.98 mrad,对应于波长的1/286。锁相残差并没有随通道数量的增加而恶化,表明该系统可以实现多通道激光放大器CBC的相位稳定锁定。相位稳定后的输出功率曲线如图3(a)所示,平均功率为776 W,对应的合成效率约为89%,在60 s内其均方根误差(RMS)为0.59%。

图4展示了全功率放大下合束后的光谱。合束后光束的3 dB带宽为9.5 nm,10 dB带宽为13.9 nm,变换极限脉冲宽度为190 fs。全功率放大下的近场光斑如图5所示。由于不同通道之间的光纤结构和放大后光束准直的差异,各通道的光斑尺寸和形状存在一定差异。由于棒状光子晶体光纤本身的特点,光斑呈现出趋于六边形的结构。然而,这些差异在合束后消失,形成了圆形的高斯光束。

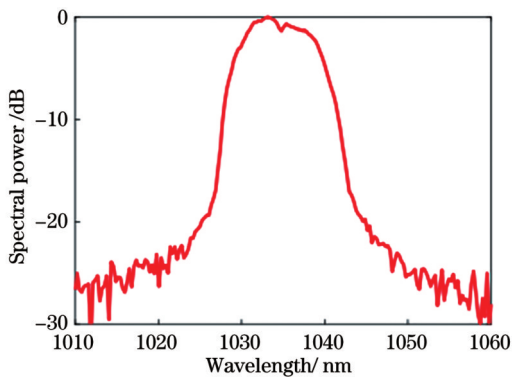


图4 全功率放大下合成光束的光谱

Fig. 4 Spectrum of combined beam under full power amplification

合成后的光束在经过脉冲压缩后,平均输出功率

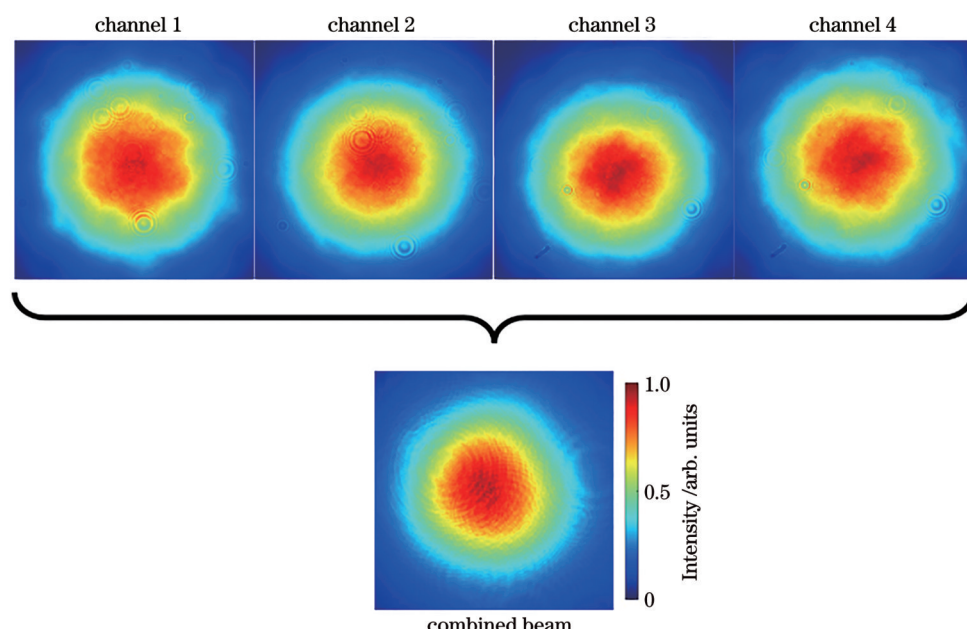


图5 全功率放大下各通道的光斑及合成光束的光斑

Fig. 5 Beam profiles of the individual channels and after coherent combination of all channels at full power amplification

为724 W,对应的单脉冲能量为905 μJ ,压缩效率约为93.3%。压缩后,<1%功率的光束通过采样镜的采样并入射到自制的SHG-FROG系统中,进行脉冲时域特性诊断,测量和重构结果如图6所示。重构使用的网格大小为 512×512 ,重构误差为0.61%。尽管通过精细调节光栅的角度和间距,压缩后脉冲宽度的半峰全宽

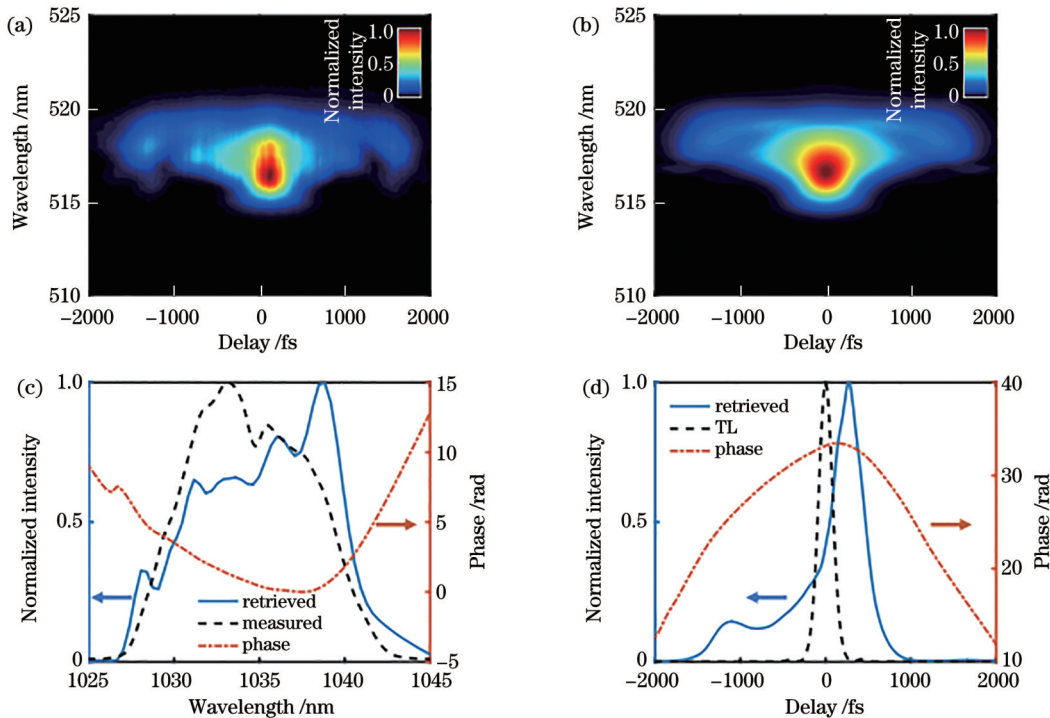


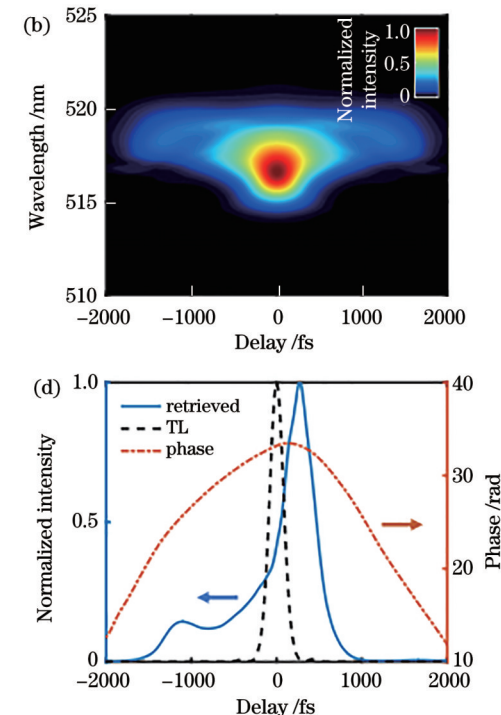
图6 仅通过光栅进行色散补偿后的脉冲特性测量。(a)实验测得的FROG行迹图;(b)重构所得的FROG行迹图;(c)实验测得的光谱(虚线)、重构所得的光谱(实线)以及光谱相位(点划线);(d)重构所得的时域脉冲包络(实线)、时域相位(点划线),以及傅里叶变换极限时域脉冲包络(虚线)

Fig. 6 Measurement of pulse characteristics after dispersion compensation by grating only. (a) Measured FROG trace; (b) retrieved FROG trace; (c) measured spectrum (dashed line), retrieved spectrum (solid line), and phase (dot dash line); (d) retrieved temporal envelope (solid line), temporal phase (dot dash line), and Fourier transform-limited temporal envelope (dashed line)

为了优化压缩脉冲的时域特性,使用TPSR对压缩后脉冲残存的高阶色散进行精确补偿。优化后的SHG-FROG测试结果如图7所示,其中重构所用的网格大小为 512×512 ,重构误差为0.39%。如图7(d)所示,脉冲宽度被进一步压缩至227 fs。通过分析图7(c)中的光谱相位,发现残存的2阶色散减小至 $1.39 \times 10^{-2} \text{ ps}^2$,3阶色散减小至 $-9.09 \times 10^{-4} \text{ ps}^3$,4阶色散减少至 $-6.08 \times 10^{-5} \text{ ps}^4$ 。相较于没有使用TPSR进行色散补偿的情况,高阶色散均显著减少,脉冲压缩效果得到明显改善。优化后的脉冲仍然存在一定的本底,这主要受到目前TPSR精度的限制,但在未使用光谱整形的条件下,依然取得了<230 fs的超短脉冲。在后续的工作中,通过严格控制各级放大器的色散管理,有望进一步优化输出脉冲质量。

最后,使用 4σ 方法测量了压缩后合成光束的质量因子 M^2 ,如图8所示。输出光束表现出接近衍射极限的光束质量,分别为 $M_x^2=1.17$ 和 $M_y^2=1.21$,插图中的

(FWHM)为445 fs,与傅里叶极限脉宽存在较大差异。从图6(c)中的光谱相位曲线可以看到仍有较多色散未补偿,这些色散导致压缩后的脉冲中有较多能量分布在波形本底中,如图6(d)所示。对光谱相位曲线的定量分析可知,残余的2阶色散为 $6.99 \times 10^{-2} \text{ ps}^2$,3阶色散为 $-5.83 \times 10^{-3} \text{ ps}^3$,4阶色散为 $1.55 \times 10^{-4} \text{ ps}^4$ 。



焦点光斑也表现出良好的高斯光束轮廓。

4 结 论

本文提出了一种基于相干光束合成的超快飞秒激光系统。通过四通道相干光束合成,系统的单脉冲能量为0.9 mJ,平均输出功率为724 W,突破了单个棒状光子晶体光纤的功率限制。通过主动的相位稳定系统,系统合成效率达到89%,且合成光束保持了良好的光束质量($M^2 < 1.25$)。此外,利用TPSR对脉冲色散进行预管理,实现了对压缩后脉冲残余色散的精确补偿,成功将脉冲宽度从445 fs优化至227 fs。该系统展示了相干光束合成在实现高平均功率和大脉冲能量飞秒激光方面的有效潜力。未来,通过增加激光脉冲的啁啾展宽量、降低重复频率以及采用时间-空间相干光束合成等手段,有望进一步提升激光脉冲的峰值功率和能量。

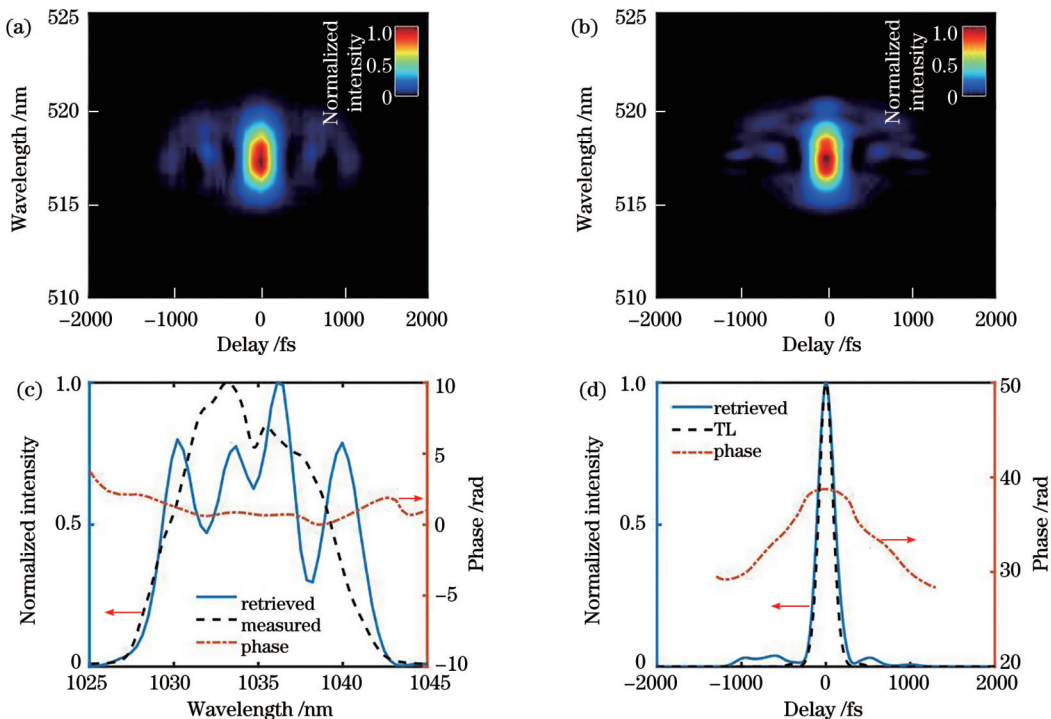


图7 使用TPSR进行精确高阶色散补偿后的脉冲特性测量。(a)实验测得的FROG行迹图;(b)重构所得的FROG行迹图;(c)实验测得的光谱(虚线)、重构所得的光谱(实线)以及光谱相位(点划线);(d)重构所得的时域脉冲包络(实线)、时域相位(点划线),以及傅里叶变换极限时域脉冲包络(虚线)

Fig. 7 Measurement of pulse characteristics after accurate high-order dispersion compensation using TPSR. (a) Measured FROG trace; (b) retrieved FROG trace; (c) measured spectrum (dashed line), retrieved spectrum (solid line), and phase (dot dash line); (d) retrieved temporal envelope (solid line), temporal phase (dot dash line), and Fourier transform-limited temporal envelope (dashed line)

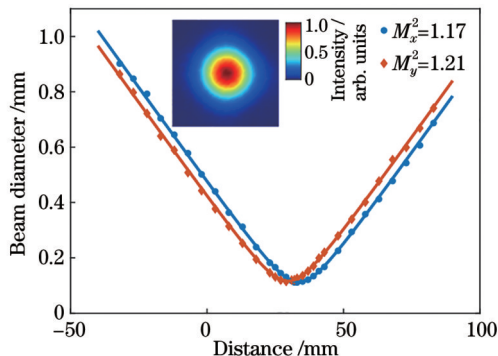


图8 全功率放大下合成光束压缩后的 M^2 (插图为焦点光束轮廓)

Fig. 8 M^2 after compression of the combined beam under full power amplification (inset is profile of focus beam)

参 考 文 献

- [1] Lorek E, Larsen E W, Heyl C M, et al. High-order harmonic generation using a high-repetition-rate turnkey laser[J]. The Review of Scientific Instruments, 2014, 85(12): 123106.
- [2] Krebs M, Hädrich S, Demmler S, et al. Towards isolated attosecond pulses at megahertz repetition rates[J]. Nature Photonics, 2013, 7: 555-559.
- [3] Buldt J, Mueller M, Stark H, et al. Fiber laser-driven gas plasma-based generation of THz radiation with 50-mW average power[J]. Applied Physics B, 2020, 126(1): 2.
- [4] Bergner K, Müller M, Klas R, et al. Scaling ultrashort laser pulse induced glass modifications for cleaving applications[J]. Applied Optics, 2018, 57(21): 5941-5947.
- [5] 魏子娟, 高熙泽, 孟翔宇, 等. 高重复频率、高功率高次谐波极紫外光源进展及应用[J]. 中国激光, 2024, 51(7): 0701001. Wei Z J, Gao X Z, Meng X Y, et al. High harmonic extreme ultraviolet light source with high repetition rate and power[J]. Chinese Journal of Laser, 2024, 51(7): 0701001.
- [6] Liang J T, Zhou Y M, Liao Y J, et al. Direct visualization of deforming atomic wavefunction in ultraintense high-frequency laser pulses[J]. Ultrafast Science, 2022, 2022: 9842716.
- [7] Dannecker B, Negel J P, Loescher A, et al. Exploiting nonlinear spectral broadening in a 400 W Yb: YAG thin-disk multipass amplifier to achieve 2 mJ pulses with sub-150 fs duration[J]. Optics Communications, 2018, 429: 180-188.
- [8] Wang T, Li C, Ren B, et al. High-power femtosecond laser generation from an all-fiber linearly polarized chirped pulse amplifier[J]. High Power Laser Science and Engineering, 2023, 11: e25.
- [9] Mason P, Divoký M, Ertel K, et al. Kilowatt average power 100 J-level diode pumped solid state laser[J]. Optica, 2017, 4(4): 438-439.
- [10] 肖虎, 李瑞晶, 吴函炼, 等. 高功率高光束质量级联泵浦掺镱光纤激光器研究进展[J]. 光学学报, 2023, 43(17): 1714009. Xiao H, Li R X, Wu H S, et al. Research progress in tandem-pumped high-power and high-beam quality ytterbium-doped fiber laser[J]. Acta Optica Sinica, 2023, 43(17): 1714009.
- [11] 吴与伦, 李丹, 等. 高功率线偏振掺镱光纤激光器性能调控技术研究进展[J]. 光学学报, 2023, 43(15): 1514001.

- Yan P, Wu Y L, Li D, et al. Performance control techniques of high-power linearly polarized Yb-doped fiber lasers[J]. *Acta Optica Sinica*, 2023, 43(15): 1514001.
- [12] Zuo J X, Lin X C. High-power laser systems[J]. *Laser & Photonics Reviews*, 2022, 16(5): 2100741.
- [13] Fathi H, Närhi M, Gumenyuk R. Towards ultimate high-power scaling coherent beam combining of fiber lasers[J]. *Photonics*, 2021, 8(12): 566.
- [14] 王小林, 文榆钧, 张汉伟, 等. 变纤芯直径掺镱光纤激光器: 现状与趋势[J]. 中国激光, 2022, 49(21): 2100001.
- Wang X L, Wen Y J, Zhang H W, et al. Ytterbium-doped core-diameter-variable fiber laser: current situation and development[J]. *Chinese Journal of Lasers*, 2022, 49(21): 2100001.
- [15] Eidam T, Rothhardt J, Stutzki F, et al. Fiber chirped-pulse amplification system emitting 3.8 GW peak power[J]. *Optics Express*, 2011, 19(1): 255-260.
- [16] Strickland D, Mourou G. Compression of amplified chirped optical pulses[J]. *Optics Communications*, 1985, 56(3): 219-221.
- [17] Krupa K, Tonello A, Shalaby B M, et al. Spatial beam self-cleaning in multimode fibres[J]. *Nature Photonics*, 2017, 11: 237-241.
- [18] He W T, Peng S X, Hu F L, et al. Cascaded Kerr beam self-cleaning in graded-index multimode fibers[J]. *Optics & Laser Technology*, 2024, 171: 110450.
- [19] 周朴, 裴荣涛, 马阎星, 等. 主动相位控制光纤激光相干合成技术研究[J]. 光学学报, 2023, 43(17): 1700001.
- Zhou P, Su R T, Ma Y X, et al. Coherent beam combining of fiber lasers by actively phase control[J]. *Acta Optica Sinica*, 2023, 43(17): 1700001.
- [20] 常洪祥, 斯凯凯, 张雨秋, 等. 基于光谱滤波的宽谱激光相干合成光程与相位同步控制研究[J]. 光学学报, 2023, 43(17): 1714008.
- Chang H X, Jin K K, Zhang Y Q, et al. Research on optical path and phase simultaneous control in coherent beam combining of broadband laser based on spectral filtering[J]. *Acta Optica Sinica*, 2023, 43(17): 1714008.
- [21] Yu C X, Augst S J, Redmond S M, et al. Coherent combining of a 4 kW, eight-element fiber amplifier array[J]. *Optics Letters*, 2011, 36(14): 2686-2688.
- [22] Wang X, Leng J, Zhou P, et al. 1.8-kW simultaneous spectral and coherent combining of three-tone nine-channel all-fiber amplifier array[J]. *Applied Physics B*, 2012, 107(3): 785-790.
- [23] Su R T, Zhou P, Ma Y X, et al. 1.2 kW average power from coherently combined single-frequency nanosecond all-fiber amplifier array[J]. *Applied Physics Express*, 2013, 6(12): 122702.
- [24] Dianault L, Hanna M, Lombard L, et al. Coherent combining of two femtosecond fiber chirped pulse amplifiers[J]. *Optics Letters*, 2011, 36(5): 621-624.
- [25] Siiman L A, Chang W Z, Zhou T, et al. Coherent femtosecond pulse combining of multiple parallel chirped pulse fiber amplifiers [J]. *Optics Express*, 2012, 20(16): 18097-18116.
- [26] Müller M, Kienel M, Klenke A, et al. 1 kW 1 mJ eight-channel ultrafast fiber laser[J]. *Optics Letters*, 2016, 41(15): 3439-3442.
- [27] Stark H, Buldt J, Müller M, et al. 1 kW, 10 mJ, 120 fs coherently combined fiber CPA laser system[J]. *Optics Letters*, 2021, 46(5): 969-972.
- [28] Stark H, Benner M, Buldt J, et al. Pulses of 32 mJ and 158 fs at 20-kHz repetition rate from a spatiotemporally combined fiber laser system[J]. *Optics Letters*, 2023, 48(11): 3007-3010.
- [29] Peng S X, Wang Z H, Hu F L, et al. 260 fs, 403 W coherently combined fiber laser with precise high-order dispersion management[J]. *Frontiers of Optoelectronics*, 2024, 17(1): 3.
- [30] Gao G, Zhang H T, Deng D C, et al. Gain effect and amplification characteristics analysis in fiber chirped pulse amplification systems[J]. *Journal of Optics*, 2018, 20(7): 075501.
- [31] Hansch T W, Couillaud B. Laser frequency stabilization by polarization spectroscopy of a reflecting reference cavity[J]. *Optics Communications*, 1980, 35(3): 441-444.

724 W, 0.9 mJ, 227 fs Four-Channel Coherently Combined Ultrafast Fiber Laser System (Invited)

Wang Zhihao¹, Peng Shuangxi¹, Xu Hao¹, Li Zhengyan², Zhang Qingbin^{1,3*}, Lu Peixiang^{1,3}

¹Wuhan National Laboratory for Optoelectronics and School of Physics, Huazhong University of Science and Technology, Wuhan 430074, Hubei, China;

²School of Optical and Electronic Information, Huazhong University of Science and Technology, Wuhan 430074, Hubei, China;

³Optics Valley Laboratory, Wuhan 430074, Hubei, China

Abstract

Objective High-average-power and high-repetition-rate femtosecond fiber lasers are widely used in industrial and scientific domains. However, the presence of excessive nonlinearity and transverse mode instability poses a constraint on further scaling of energy and power within the fiber lasers. Coherent beam combination (CBC) has risen as a viable solution to the constraint, enabling the extension of average power and pulse energy limits while preserving beam quality. Under ideal conditions, the laser power and energy of the combined beam from N channels can reach N times that of a single amplifier. However, in real-world applications, variations in beam quality and discrepancies in the spatiotemporal properties of the beams result in power losses during the combining process. These losses are quantified by the combining efficiency. Recently, an average power of 1 kW with a pulse energy of 1 mJ and an average power of 1 kW with a single

pulse energy of 10 mJ are achieved through 8-channel and 16-channel fiber laser CBC, respectively. Yet, the proliferation of combination paths not only increases system complexity but also affects stability. Moreover, due to gain narrowing and incomplete dispersion compensation, compressed pulses typically exceed 300 fs, presenting hurdles in achieving Fourier limit pulse duration. Although methods such as spectral shaping and post-compression can further shorten the pulse duration, these methods undoubtedly further increase the complexity and operational difficulty of the system. Hence, we focus on reducing the number of combination paths and improving dispersion compensation to achieve clean ultrashort femtosecond pulses while maintaining the existing power level.

Methods To streamline the number of combination paths, enhancing the power of a single amplifier is crucial. By boosting the power of a single amplifier beyond 200 W, the number of required combination channels can be reduced by a factor of 2 to 3. An ultrafast femtosecond fiber system comprising four coherently combined large mode-area rod-type photonic crystal fibers as the main amplifier is constructed. To ensure high beam combining efficiency and subsequent high-quality pulse compression, it is necessary to strictly control the power of each amplifier to ensure the same B-integral. Meanwhile, due to the effect of nonlinear polarization rotation, a large amount of laser power cannot participate in beam combination. Circularly polarized amplification is an effective method to minimize nonlinear phase accumulation and ensure high beam combining power. The phase stabilization is achieved using Hänsch-Couillaud (HC) detectors after beam combination. While spectral pre-shaping of seed light is effective for optimizing the duration of compressed pulses, its practical operation is cumbersome. Hence, we use the tunable pulse stretcher (TPSR) to pre-compensate the dispersion of the seed light. This matches the pre-compensate dispersion with the accumulated dispersion during subsequent amplification and compression processes, further optimizing the pulse duration.

Results and Discussions The average output power of each channel ranges from 215 to 222 W, with a fitted slope efficiency exceeding 65%. The maximum discrepancy between the channels is no greater than 3%. This precision enables our four-channel CBC system to achieve an output power of 776 W with a pulse energy of 0.97 mJ, and a combination efficiency of 89%. The active phase stabilization system ensures excellent power stability for the four-channel CBC fiber lasers, with a root mean square of 0.59%. Despite the differences in the output beam profiles of different channels, the combined beam still exhibits a circular Gaussian profile. The beam quality is analyzed by M^2 measurement using the 4σ -method showing an almost diffraction limit beam quality of $M^2 < 1.25$ on both axes. Remarkably, we accomplish these results using only four amplifiers, whereas previous researchers required eight or more, effectively reducing system complexity. After compression by gratings, the combined beam exhibits a pulse duration of 445 fs and significant high-order dispersion residue, as shown in Fig. 6. By optimizing dispersion, particularly high-order dispersion, using TPSR, we reduce the pulse duration to 227 fs and significantly increase the proportion of main pulse energy, as illustrated in Fig. 7. Spectral phase analysis shows a significant reduction in second to fourth order dispersion. The compression efficiency reaches 93.3%, with compressed power at 724 W and pulse energy at 0.9 mJ.

Conclusions We present an ultrafast femtosecond laser system based on CBC. The system achieves an average power of 724 W and a pulse energy of 0.9 mJ through CBC of four channels. This approach effectively overcomes the power limitation of a single rod-type photonic crystal fiber. By employing an active phase stabilization system, the combination efficiency of the system reaches 89%, while the combined beam maintains good beam quality with $M^2 < 1.25$. Furthermore, the use of TPSR for pre-management of pulse dispersion enables precise compensation of the residual dispersion after pulse compression, successfully optimizing the pulse duration full width at half maximum (FWHM) from 445 to 227 fs. The system demonstrates the effective potential of coherent beam combining in achieving high average power and large pulse energy femtosecond lasers. In the future, it is expected that by increasing the chirp broadening of pulses, reducing the repetition rate, and incorporating spatial-temporal coherent beam combining, the peak power and energy of laser pulses can be further enhanced.

Key words ultrafast fiber laser; coherent beam combination; chirped pulse amplification; dispersion compensation